

Defect Reduction Treatment for Plasma–Tetraethylorthosilicate–SiO₂ by High-Pressure H₂O Vapor Heat Treatment

Hajime WATAKABE, Toshiyuki SAMESHIMA, Thomas STRUTZ¹, Teruki OITOME¹ and Atsushi KOHNO²

Department of Electrical and Electronic Engineering, Tokyo University of Agriculture and Technology, Tokyo 184-8588, Japan

¹*UNAXIS Japan, Osaka 564-0037, Japan*

²*Department of Applied Physics, Fukuoka University, Fukuoka 814-0180, Japan*

(Received May 25, 2005; accepted August 23, 2005; published December 8, 2005)

Improvements in the electrical and structural properties of tetraethylorthosilicate (TEOS) SiO₂ films fabricated by plasma-enhanced chemical vapor deposition (PECVD) method were investigated using high-pressure H₂O vapor heat treatment. The density of interface trap states was reduced from 3.3×10^{12} (initial) to $5.1 \times 10^{10} \text{ cm}^{-2} \text{ eV}^{-1}$ by $1.3 \times 10^6 \text{ Pa}$ H₂O vapor heat treatment at 260°C for 9 h. The density of fixed charges was also reduced from 6.1×10^{11} to $1.3 \times 10^{11} \text{ cm}^{-2}$. The full width at half-maximum (FWHM) of the optical absorption band corresponding to vibration of Si–O–Si bonding was reduced from 82.9 to 78.1 cm⁻¹. Narrowing in FWHM of the Si 2p core level peak measured by X-ray photoelectron spectroscopy (XPS) was also observed. The reduction in the FWHM probably results from improvement of the Si–O bonding network.

[DOI: 10.1143/JJAP.44.8367]

KEYWORDS: TEOS–SiO₂, H₂O vapor heat treatment, interface trap states, optical absorption peaks, XPS

1. Introduction

Formation of SiO₂ films by plasma-enhanced chemical vapor deposition (PECVD) using tetraethylorthosilicate (TEOS) has been used and investigated for integrated circuit device fabrication such as internal isolation dielectric layers and as passivation layers because of excellent step coverage.^{1–5)} Recently, TEOS–SiO₂ has been used for low-temperature fabrication of polycrystalline-silicon thin-film transistors (poly-Si TFTs) as a gate insulator.^{6,7)} The formation of a TEOS–SiO₂/poly-Si interface with a low defect density is important because TFT characteristics are seriously governed by electrical interface properties.^{8–10)} We previously reported that high-pressure H₂O vapor heat treatment effectively improved thermal-evaporated SiO_x films as well as the SiO_x/Si interface.^{11–14)} TFT characteristics were also improved by the H₂O vapor heat treatment after TFT fabrication.^{15,16)}

In this paper, we report improvements in the electrical and structural properties of TEOS–SiO₂ as well as its interface by high-pressure H₂O vapor heat treatment. Reduction in the density of SiO₂/Si interface trap states, estimated from capacitance vs voltage (*C–V*) characteristics, using the H₂O vapor heat treatment is presented. Improvement of the Si–O bonding network using Fourier transform infrared spectrometry (FT-IR) is reported. Change in the Si 2p core level spectra measured by X-ray photoelectron spectroscopy (XPS) is also discussed.

2. Experimental

SiO₂ films with thicknesses of 50 and 100 nm were formed on N-type (100) single-crystalline silicon substrates with a resistivity of 10 Ω cm by PECVD at 330°C using TEOS–O₂ mixed gases with Ar carrier gas. The thicknesses of the TEOS–SiO₂ films were measured by spectroscopic ellipsometry. Al gate electrodes with an area of 0.01 cm² were formed on the TEOS–SiO₂ surface by thermal evaporation in order to form a metal–oxide–semiconductor (MOS) capacitor structure. Heat treatment with $1.3 \times 10^6 \text{ Pa}$ –H₂O vapor was then carried out at 200 and 260°C for 3 and 9 h. The thickness of TEOS–SiO₂ films was not changed

by the H₂O vapor heat treatment.

SiO₂/Si interface properties of the MOS capacitors were analyzed by high-frequency (100 kHz) and low-frequency (quasi-static) *C–V* characteristics. The density of interface trap states near the midgap, *D*_{it}, was determined by the difference between capacitances resulting from high- and low-frequency gate voltage application at the weak inversion as shown by the following equation,¹⁷⁾

$$D_{it} = \frac{C_{ox}}{q} \left(\frac{C_{lf}/C_{ox}}{1 - C_{lf}/C_{ox}} - \frac{C_{hf}/C_{ox}}{1 - C_{hf}/C_{ox}} \right), \quad (1)$$

where *C*_{ox} is the capacitance of SiO₂ film per unit area, *C*_{lf} is the minimum capacitance per unit area in the low-frequency *C–V* characteristics, *C*_{hf} is the capacitance per unit area in the high-frequency *C–V* characteristics at the gate voltage giving *C*_{lf}, and *q* is the elemental charge. In this study, the density of interface trap states was estimated at an energy level of 0.50 eV from the valence band edge. Current density vs electrical field (*J–E*) characteristics were also measured using the MOS capacitors with 50-nm-thick TEOS–SiO₂ films. The electrical field was applied to the TEOS–SiO₂ films by gate voltage application from 0 to 50 V with 0.25 V steps. The optical absorption spectra were measured using FT-IR (JASCO FT/IR 6100) in the wave number range between 400 and 4000 cm⁻¹ with a resolution of 4 cm⁻¹. The optical absorption spectra were carefully measured in vacuum at 100 Pa in order to avoid the contribution of H₂O molecules in air. The absorbance of SiO₂ films was obtained by subtracting the absorption of silicon using the unprocessed crystalline silicon wafers. Bonding states in the SiO₂ were analyzed by XPS with an ESCA Model-1800L (ULVAC-PHI) using monochromatic Al Kα radiation (1486.6 eV). The C 1s core level spectra from carbon adsorbed on the SiO₂ film were used for energy adjustment at a binding energy of 284.5 eV, since the binding energy was calibrated in advance using the Au 4f_{7/2} core level peak (84.0 eV) after which the C 1s peak position from carbon on the Au corresponded to 284.5 eV. The Au 4f_{7/2} and 4f_{5/2} spin-orbit doublet was separated by 3.68 eV. The Si 2p peak was fitted to a pseudo-Voigt function by the least-squares method in order to evaluate the peak position and full width at half-maximum (FWHM).

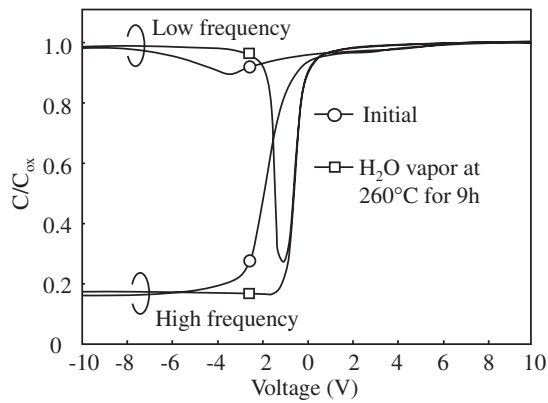


Fig. 1. High-frequency (100 kHz) and low-frequency (quasi-static) C - V characteristics for N-type MOS capacitors with 50-nm-thick TEOS-SiO₂ films as fabricated and treated with 1.3×10^6 Pa H₂O vapor heat treatment at 260°C for 9h.

3. Results and Discussion

Figure 1 shows high- and low-frequency C - V characteristics for 50-nm-thick TEOS-SiO₂ films as fabricated and treated with H₂O vapor at 260°C for 9h. In the high-frequency C - V characteristic for initial SiO₂ film, the normalized capacitance gradually increased as gate voltage increased from -6 to 2 V. A large capacitance difference between high- and low-frequency C - V characteristics was observed in the weak inversion region at around -4 V. This indicates that there was a high defect density at the SiO₂/Si interface. On the other hand, the capacitance in the high-frequency C - V characteristics steeply increased as the gate voltage increased from -1 to 1 V after H₂O vapor heat treatment. The capacitance for low-frequency C - V characteristics was markedly reduced at gate voltages between -2 and 0 V and became close to that for high-frequency C - V characteristics at around -1 V. This means that H₂O vapor heat treatment reduced electrically active defects at the SiO₂/Si interface. Moreover, the H₂O vapor heat treatment reduced the negative voltage shift of the C - V curve caused by the positive fixed charges.

Figure 2 shows the densities of interface trap states (a) and positive fixed charges (b) as functions of the duration of H₂O vapor heat treatment at 200 and 260°C. The density of interface trap states for initial SiO₂ film was evaluated to be 3.3×10^{12} cm⁻² eV⁻¹. H₂O vapor heat treatment reduced the density of interface trap states with increasing treatment duration. The interface trap state density was effectively decreased to 5.1×10^{10} cm⁻² eV⁻¹ by the treatment at 260°C for 9h. The density of fixed charges was also reduced from 6.1×10^{11} (initial) to 1.3×10^{11} cm⁻² by the treatment for 9h, as shown in Fig. 2(b).

Figure 3 shows J - E characteristics for MOS capacitors with 50-nm-thick TEOS-SiO₂ films for as fabricated and H₂O vapor heat treatment cases. In electrical fields lower than 6 MV/cm, the current density for every sample was lower than 10^{-8} A/cm² and no significant change in the J - E curve due to the H₂O vapor heat treatment was observed. On the other hand, in electrical fields higher than 6 MV/cm, the current density markedly increased as the electrical field increased. From the results of the fitting process between experimental and theoretical J - E curves, the carrier trans-

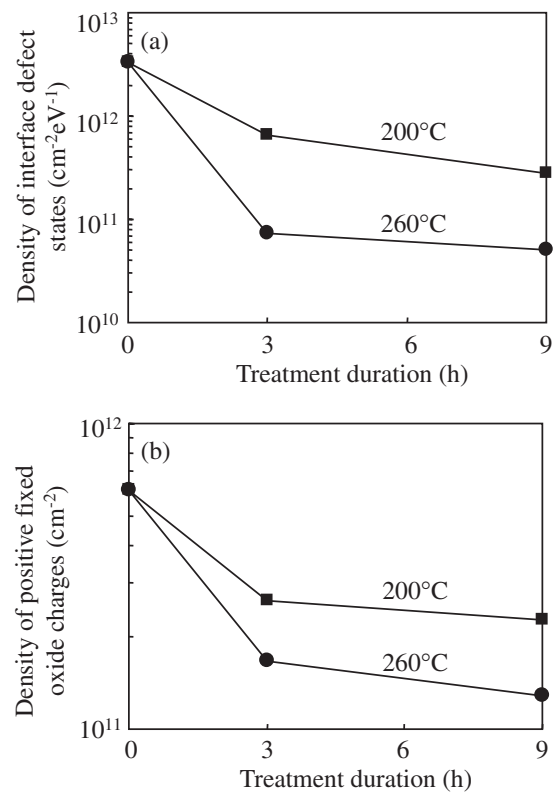


Fig. 2. Densities of interface defect states (a) and positive fixed oxide charges (b) as functions of duration of H₂O vapor heat treatment at 200 and 260°C. The density of interface defect states was estimated from the difference between capacitances resulting from high- and low-frequency gate voltage application at the weak inversion region.

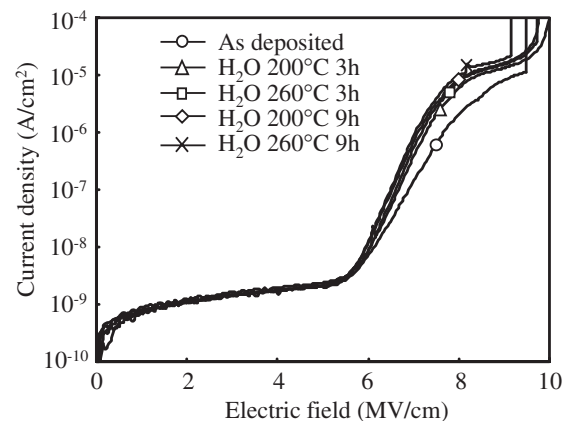


Fig. 3. J - E characteristics for N-type MOS capacitors with 50-nm-thick TEOS-SiO₂ films as fabricated and treated with H₂O vapor. The electrical field was applied to the TEOS-SiO₂ films by gate voltage application from 0 to 50 V with 0.25 V steps.

port was governed by the Poole-Frenkel (PF) conduction in the electrical field between 6 and 7 MV/cm described as^{18,19)}

$$J = C_1 E \exp\{-q[\phi - (qE/\pi\epsilon_0\epsilon_r)^{1/2}]/kT\}, \quad (2)$$

where C_1 is a constant proportional to the trap density, E is the electric field, q is the elemental charge, ϕ is the barrier height, ϵ_0 is the permittivity of free space, ϵ_r is the specific dielectric constant, k is the Boltzmann constant and T is the absolute temperature. The current density was increased by

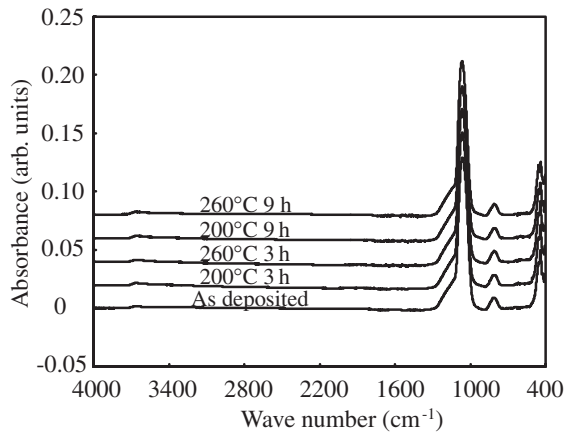


Fig. 4. Optical absorption spectra in infrared region measured using FT-IR for films as fabricated and treated with H₂O vapor. The absorption spectra were measured in vacuum at 100 Pa.

the H₂O vapor treatment in high electrical fields. The current density was increased from 6.5×10^{-8} (initial) to 6.0×10^{-7} A/cm² at 7 MV/cm by H₂O vapor heat treatment at 260°C for 9 h. The carrier transport was still interpreted by the PF conduction.

Figure 4 shows absorption spectra in the infrared region for 100-nm-thick TEOS-SiO₂ films as fabricated and treated with H₂O vapor. Large absorption peaks corresponding to Si-O-Si antisymmetric stretching at 1064 cm⁻¹, bending at 820 cm⁻¹ and rocking at 470 cm⁻¹ vibration modes were observed. Small absorption peaks corresponding to Si-O-H bonding were observed for all samples at around 3650 cm⁻¹.^{1,7)}

Figure 5 shows the changes in the FWHM of absorption peaks corresponding to the Si-O-Si antisymmetric stretching vibration mode as a function of the duration of H₂O vapor heat treatment at 200 and 260°C obtained from Fig. 4. The FWHM for initial SiO₂ film was 82.9 cm⁻¹, which was larger than that of thermally grown SiO₂, 69 cm⁻¹.¹¹⁾ The FWHM was reduced to 78.1 cm⁻¹ as treatment duration increased to 9 h for the temperature of 260°C. Peak wave number was also slightly increased from 1061 (initial) to 1065 cm⁻¹ as treatment duration increased to 9 h for both temperatures of 200 and 260°C. These results indicate that H₂O vapor heat treatment reduced the distribution of the Si-O-Si bonding angle. The density of Si-O weak bonds in SiO₂ films was probably reduced by hydrolytic chemical reaction with H₂O molecules so that Si-O bonding homogeneity was achieved. We hypothesize that this reduction in the weak bond density resulted in the decrease in the densities of trap states at SiO₂/Si interface and fixed charges as shown in Figs. 2(a) and 2(b). Figure 6 shows total absorbance integrated from 3450 to 3730 cm⁻¹ corresponding to the Si-O-H bonding as a function of the duration of H₂O vapor heat treatment at 200 and 260°C obtained from Fig. 4. The total absorbance increased as treatment duration increased for each temperature case. The Si-O-H bonding formed by the H₂O vapor heat treatment uniformly distributed in the films because the total absorbance corresponding to the Si-O-H bonding for 50-nm-thick TEOS-SiO₂ film treated with H₂O vapor at 260°C for 9 h was 0.53 times that for the 100 nm film. There was a possibility that

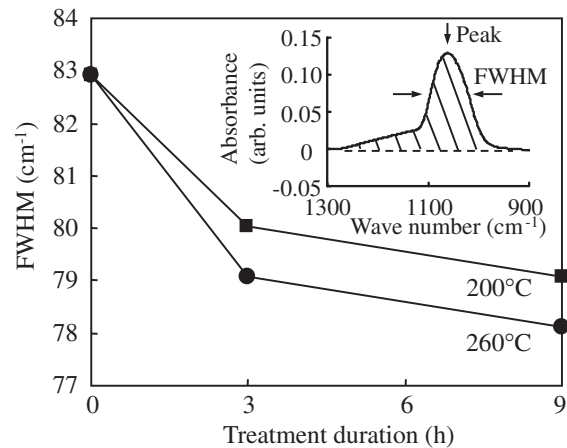


Fig. 5. Changes in FWHM of absorption peak corresponding to Si-O bonding as a function of duration of H₂O vapor heat treatment at 200 and 260°C obtained from Fig. 4.

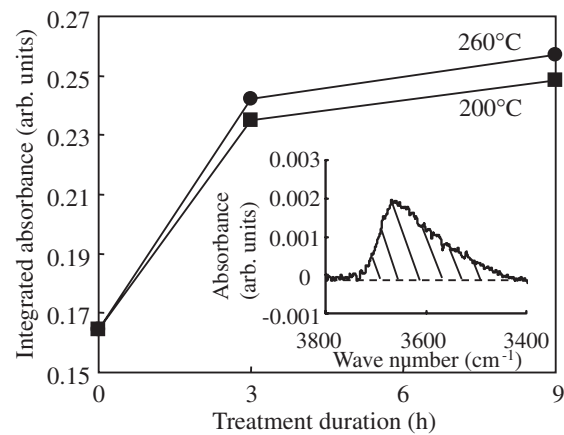


Fig. 6. Total absorbance integrated from 3450 to 3730 cm⁻¹ corresponding to Si-O-H bonding as a function of duration of H₂O vapor heat treatment at 200 and 260°C obtained from Fig. 4.

Si-O-H bonding also reduced the densities of positive fixed charges and interface trap states via termination of Si dangling bonds on the basis of the results shown in Figs. 2 and 6. However, there was also a possibility that Si-O-H bonding became leakage sites in the SiO₂ on the basis of the results shown in Figs. 3 and 6. Those Si-O-H leakage sites in the SiO₂ films probably increased the PF current in high electrical fields as shown in Fig. 3. From the fitting process, the density of trap sites of the TEOS-SiO₂ film treated with H₂O vapor at 260°C for 9 h was 9.2 times larger than that of the initial film.

Figure 7 shows peak energy (a) and FWHM (b) for Si 2p core level peaks determined by XPS as a function of the duration of H₂O vapor heat treatment at 200 and 260°C. The thermally grown SiO₂ films with a thickness of 100 nm were also treated under the same condition and measured for reference. From the results of the C-V measurement, the densities of fixed oxide charges and interface trap states of thermally grown SiO₂ films were estimated to be 1.2×10^{11} cm⁻² and 4.0×10^{10} cm⁻² eV⁻¹, respectively. These values were not changed by the H₂O vapor heat treatment. The peak energy of 103.56 eV for initial TEOS-SiO₂ film was

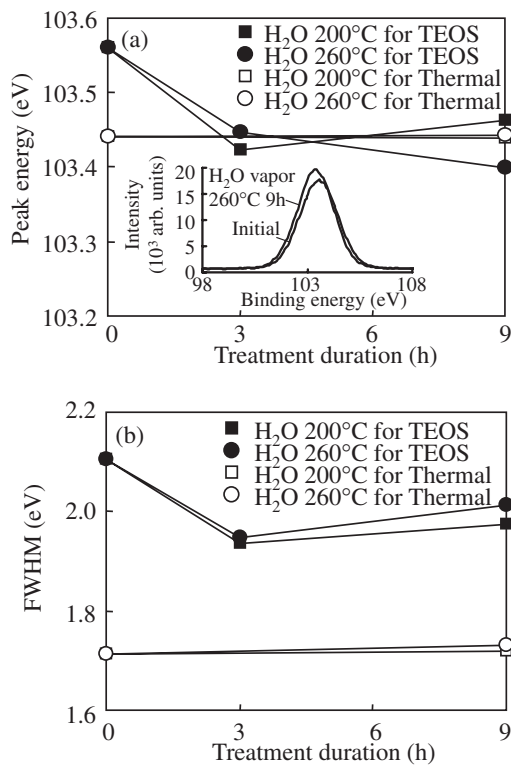


Fig. 7. Peak energy (a) and FWHM (b) for Si 2p core level peak in TEOS-SiO₂ as functions of duration of H₂O vapor heat treatment at 200 and 260°C. Thermally grown SiO₂ films were also treated under the same condition and measured for reference. The peak energy and FWHM were evaluated by the least-squares fitting method using a pseudo-Voigt function. The inset shows Si 2p XPS spectra of the TEOS-SiO₂ films as deposited and treated with H₂O vapor heat treatment at 260°C for 9 h.

higher than that of 103.44 eV for thermally grown SiO₂, as shown in Fig. 7(a). By the H₂O vapor heat treatment, although the Si 2p peak position for the thermally grown SiO₂ was not changed, the peak position for the TEOS-SiO₂ shifted to the low binding energy region and coincided with that for thermally grown SiO₂. This peak shift in the TEOS-SiO₂ film means that the Si-O bonding states were improved and/or the positive charge was reduced by the H₂O vapor heat treatment. The FWHM of the Si 2p peak for initial TEOS-SiO₂ was 2.11 eV as shown in Fig. 7(b). The peak was sharpened from 1.94 to 2.01 eV by the H₂O vapor heat treatment. The narrowing of FWHM seems to be explained by the improvement of the inhomogeneity of the Si-O bonding network in consistency with the result in Fig. 5 as described above, although the inhomogeneity caused by the differential charging effect should be considered.

4. Conclusions

Improvements in the electrical and structural properties of TEOS-SiO₂ film using high-pressure H₂O vapor heat

treatment were discussed. The density of interface defect states was analyzed by the measurement of high- and low-frequency C-V characteristics. The density of interface trap states for initial SiO₂ film was estimated to be $3.3 \times 10^{12} \text{ cm}^{-2} \text{ eV}^{-1}$. $1.3 \times 10^6 \text{ Pa}$ H₂O vapor heat treatment at 260°C for 9 h effectively reduced the density of interface trap states to $5.1 \times 10^{10} \text{ cm}^{-2} \text{ eV}^{-1}$. However, the H₂O vapor heat treatment increased the leakage current in high electrical fields above 6 MV/cm. Improvement of the Si-O bonding network was observed by FT-IR measurement. The FWHM of optical peaks corresponding to the vibration of Si-O bonding was reduced from 82.9 (initial) to 78.1 cm⁻¹. The improvement of the Si-O bonding network is probably related to the reduction in the densities of positive fixed charges and interface trap states with the reduction of Si-O weak bonds. Formation of Si-O-H bonding by the H₂O vapor heat treatment also reduced the density of positive fixed charges and interface trap states with termination of Si dangling bonds. The FWHM of the Si 2p core level peak was also narrowed by H₂O vapor heat treatment. This FWHM reduction was probably caused from the improvement of the Si-O bonding network.

- 1) S. Nguyen, D. Dobuzinsky, D. Harmon, R. Gleason and S. Fridmann: *J. Electrochem. Soc.* **137** (1990) 2209.
- 2) C. S. Pai and C. P. Chang: *J. Appl. Phys.* **68** (1990) 793.
- 3) I. T. Emesh, G. Dasti, J. S. Mercier and P. Leung: *J. Electrochem. Soc.* **136** (1989) 3404.
- 4) B. L. Chin and E. P. van de Ven: *Solid State Technol.* **31** (1988) 119.
- 5) G. W. Hills, A. S. Harrus and M. J. Thoma: *Solid State Technol.* **33** (1990) 127.
- 6) J. Chae, E. Kim, Y. S. Jung, J. I. Kim, M. S. Yang and C. D. Kim: *Jpn. J. Appl. Phys.* **43** (2004) 6937.
- 7) Y. Nishi, T. Funai, H. Izawa, T. Fujimoto, H. Morimoto and M. Ishii: *Jpn. J. Appl. Phys.* **31** (1992) 4570.
- 8) S. Higashi, D. Abe, Y. Hiroshima, K. Miyashita, T. Kawamura, S. Inoue and T. Shimoda: *Jpn. J. Appl. Phys.* **41** (2002) 3646.
- 9) A. Kohno, T. Sameshima, N. Sano, M. Sekiya and M. Hara: *IEEE Trans. Electron Devices* **42** 251 (1995).
- 10) K. M. Chang, W. C. Yang and C. P. Tsai: *IEEE Electron Device Lett.* **24** (2003) 512.
- 11) T. Sameshima and M. Satoh: *Jpn. J. Appl. Phys.* **36** (1997) L687.
- 12) T. Sameshima, K. Sakamoto, Y. Tsunoda and T. Saitoh: *Jpn. J. Appl. Phys.* **37** (1998) L1452.
- 13) T. Sameshima, K. Sakamoto and M. Satoh: *Thin Solid Films* **335** (1998) 138.
- 14) T. Sameshima, K. Sakamoto and K. Asada: *Appl. Phys. A* **69** (1999) 221.
- 15) T. Sameshima, M. Satoh, K. Sakamoto, K. Ozaki and K. Saitoh: *Jpn. J. Appl. Phys.* **37** (1998) L1030.
- 16) H. Watakabe and T. Sameshima: *Jpn. J. Appl. Phys.* **41** (2002) L974.
- 17) E. H. Nicollian and J. R. Brews: *MOS (Metal Oxide Semiconductor) Physics and Technology* (Wiley-Interscience, New York, 1982) Chap. 8, p. 332.
- 18) E. Kameda, T. Matsuda, Y. Emura and T. Ohzone: *Solid-State Electron.* **42** (1998) L2105.
- 19) S. P. Lau, J. M. Shannon and B. J. Sealy: *J. Non-Cryst. Solids* **227-230** (1998) 533.